

Rapid evolution of arginine deiminase for improved anti-tumor activity

Ye Ni · Yongmei Liu · Ulrich Schwaneberg · Leilei Zhu ·
Na Li · Lifeng Li · Zhihao Sun

Received: 21 October 2010 / Revised: 29 November 2010 / Accepted: 30 November 2010 / Published online: 11 January 2011
© Springer-Verlag 2011

Abstract Arginine deiminase (ADI), an arginine-degrading enzyme, has been studied as a potential anti-cancer agent for inhibiting arginine-auxotrophic tumors, such as melanomas and hepatocellular carcinomas. Based on our preliminary results, it was noticed that the optimum pH of ADI from *Pseudomonas plecoglossicida* (PpADI) was 6.0, and less than 10% of the activity was retained at pH 7.4 (pH of human plasma). Additionally, the K_m value for wild-type ADI (WT-ADI) was 2.88 mM (pH 6.0), which is over 20 times of the serum arginine level (100–120 μ M). These are two major limitations for PpADI as a potential anti-cancer drug. A highly sensitive and efficient high-throughput screening strategy based on a modified diacetylmonoxime–thiosemicarbazide method was established to isolate ADI mutants with higher activity and lower K_m under physiological pH. Three improved mutants was selected from 650 variants after one round of ep-PCR, among which mutant 314 (M314: A128T, H404R, I410L) exhibiting the highest activity. Interestingly, sequence alignment shows that three amino acid substitutes in M314 are coincident with corresponding residues in ADI from *Mycoplasma arginini*.

The specific activity of M314 (9.02 U/mg) is over 20-fold higher than that of WT-ADI (0.44 U/mg) at pH 7.4, and the K_m value was reduced to 0.65 mM (pH 7.4). Noticeably, the pH optimum was shifted from 6.0 to 6.5 in M314. Homology model of M314 was constructed to understand the molecular basis of the improved enzymatic properties. This work could provide promising drug candidate for curing arginine-auxotrophic cancers.

Keywords Arginine deiminase · Directed evolution · pH optimum · Anti-tumor · *Pseudomonas plecoglossicida* · Hepatocellular carcinomas

Introduction

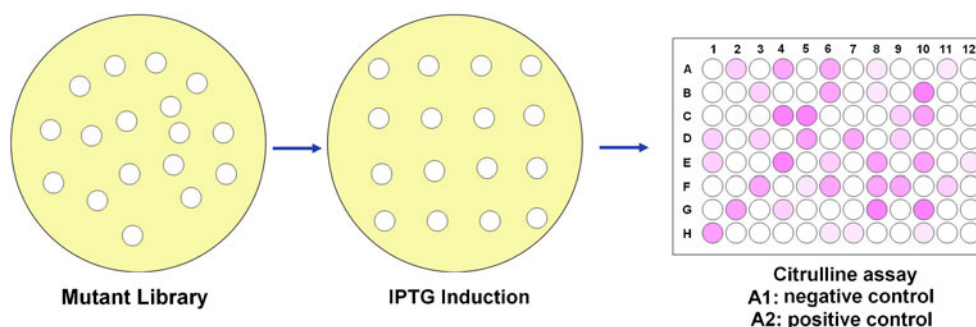
Hepatocellular carcinomas (HCCs) are fatal diseases and are highly resistant to chemotherapies. Less than 10% of HCC patients are candidates for surgical resection or transplantation (Curley et al. 2002; Ryder 2003; Watkins and Curley 2000). In the United States, approximately 20,000 new cases are diagnosed annually, with more than 18,700 deaths annually. The international yearly incidence is approximately one million cases (Izzo et al. 2004). Effective treatments for these diseases are urgently needed. However, these carcinomas have been confirmed to be arginine-auxotrophic, while normal cells can synthesize sufficient arginine for their own needs. Arginine deiminase (ADI; EC 3.5.3.6) belongs to a guanidine group-modifying enzyme superfamily and catalyzes the irreversible hydrolysis of arginine to citrulline and ammonia (Shirai et al. 2001). Thus, systemic arginine depletion by ADI is an attractive therapeutic strategy targeting malignant arginine-auxotrophic cells (Miyazaki et al. 1990; Sugimura et al. 1990, 1992; Takaku et al. 1992, 1993, 1995; Gong et al. 1999). Currently, clinical trials of ADI-PEG-20 for

Y. Ni (✉) · Y. Liu · N. Li · L. Li · Z. Sun (✉)
The Key Laboratory of Industrial Biotechnology, Ministry of
Education, Laboratory of Biocatalysis, School of Biotechnology,
Jiangnan University,
1800 Lihu Rd.,
214122, Wuxi, People's Republic of China
e-mail: yni@jiangnan.edu.cn

Z. Sun
e-mail: sunzhihao@jiangnan.edu.cn

U. Schwaneberg · L. Zhu
Lehrstuhl für Biotechnologie, RWTH Aachen University,
Worringerweg 1,
52056, Aachen, Germany

Fig. 1 Two-step procedure for the screening of PpADI with improved activity. (The purple color on 96-well microtiter plate indicates variants with ADI activity. negative control: without colonies; positive control: IPTG induced WT-ADI colonies)



the treatment of HCCs (phase III) and melanomas (phase I/II) are being investigated (Izzo et al. 2004; Shen and Shen 2006). In addition, ADI was suggested to be a potentially better treatment for leukemia than L-asparaginase and appears to have fewer side effects due to its high substrate specificity towards arginine (Gong et al. 2000). Recently, ADI-PEG-20 was reported to induce ASS-deficiency prostate cancer cells CWR22Rv1 autophagy at 0.3 $\mu\text{g}/\text{ml}$ ADI-PEG-20 (Kim et al. 2009). Studies also showed that ADI-PEG-20 is responsible for the down-regulation expression of HIF-1 α and up-regulation of c-Myc in culture melanoma. As important factors in cancer cell energy metabolism, the expression modulation of HIF-1 α and c-Myc may enhance the efficacy of ADI-PEG-20 (Kuo et al. 2010).

In our preceding study, a *Pseudomonas plecoglossicida* CGMCC2039 strain with remarkable ADI activity and in vitro anti-tumor activity was isolated and characterized (Liu et al. 2008). ADI from *P. plecoglossicida* CGMCC2039 (PpADI) was expressed in *Escherichia coli* BL21 (DE3) (Ni et al. 2009). The recombinant ADI was purified to homogeneity, and the specific activity was 4.76 U/mg (pH 6.0 and 37°C), a pH shift from 6.0 to 7.4 results in over 90% activity drop. Besides, the K_m value of WT-ADI was determined to be as high as 2.88 mM, representing more than 20 times of the serum arginine level (100–120 μM). Therefore, the potential application of PpADI as an anti-cancer drug could be greatly hampered by its low activity and high K_m value under physiological condition. Directed evolution approach experimentally modifies a biological

molecule towards a desirable property and could be performed much more rapidly and directly in evolving a molecular property where nature does not provide one. Lin et al. (2009) improved catalytic efficiency of endo- β -1,4 glucanase by directed evolution. A mutant with wider pH tolerance and enhanced activity was selected. Our collaboration group in Germany first reported the directed PpADI evolution for increased activity at physiological pH, in which the screening procedure involves liquid cultivation and induction, liquid culture transferring, and colorimetric reaction in 96-well plates (Zhu et al. 2010). The best mutant M2 with fourfold increased activity and threefold increased K_m at pH 7.4 was selected from 2,400 mutants. The use of high substrate concentration (around 100 mM arginine) is speculated to be responsible for the significantly increased K_m . Here, we report the directed evolution of PpADI using a fast and precise two-step screening procedure, in which colonies on IPTG-agar plate was subjected to activity assay directly without tedious liquid cultivation. In this study, PpADI mutants generated by ep-PCR was measured by 96-well microtiter plate assay based on a modified DAM–TSC method (Qian et al. 2007), which has better color stability, higher sensitivity and precision compared with method of Archibald (1944). Since the linearity range of DAM–TSC method was 0.02 to 1 mM, arginine concentration was dropped to 0.5 mM compared with 83 mM used in Zhu's report (2010). This high-throughput screening strategy was proven to be faster and more precise in identifying PpADI mutants with higher activity and lower K_m at physiological pH. One excellent mutant 314 (M314) was selected among 650 variants after one round of ep-PCR. The specific activity of M314 is over 20-fold higher than that of WT-ADI, and the K_m value was 0.65 mM at pH 7.4. Noticeably, the pH optimum was shifted from 6.0 to 6.5 in M314.

Table 1 Activity of PpADI mutants measured at pH 7.4 and pH 6.0 in comparison with WT-ADI

PpADI mutants	ADI activity	
	pH 6.0	pH 7.4
WT	10.9	1 ^a
M177 (V10F)	15.8	8.64
M314 (A128T,H404R,I410L)	38.0	20.5
M558 (R18L)	12.3	4.77

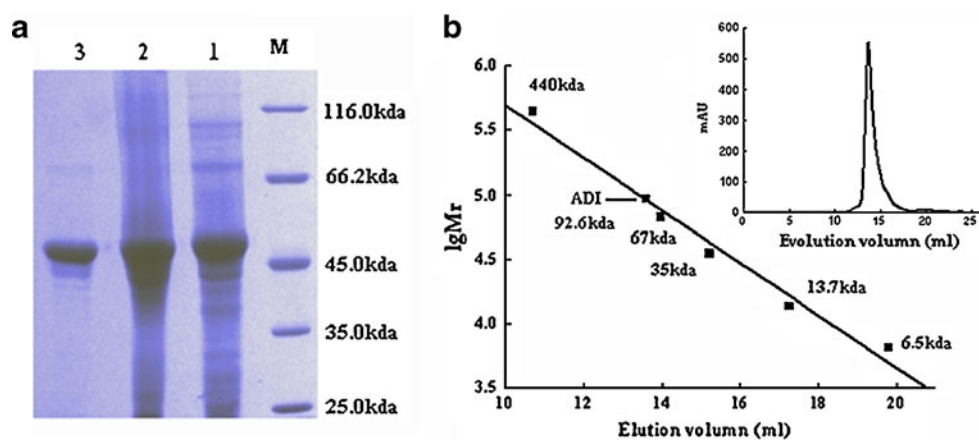
^a The activity of WT-ADI at pH 7.4 was supposed to be 1

Materials and methods

Strains and culture media

E. coli BL21 (DE3) was used as the expression host and was incubated in Luria–Bertani (LB) at 37°C.

Fig. 2 Expression and purification of M314. **a** SDS-PAGE analysis of the expressed and purified ADI from *E. coli* harboring pPADI. Lanes: *M* molecular-mass maker protein; 1 total cell extract with IPTG; 2 eluted fraction from DEAE FF-Sephacrose; 3 eluted fraction from Superdex 200. **b** Native molecular weight determination of rADI on Superdex 200 column. Protein elution profile by OD₂₈₀ is shown in the inset



Reagents

The Bradford reagent was purchased from Genaray (Shanghai, China), and other chemicals used were of reagent grade and were obtained from Sinochem Shanghai (Shanghai, China).

Acid-ferric solution (I) consists of H₂SO₄ (95%, 160 ml), H₃PO₄ (85%, 70 ml), and 0.1 g FeCl₃. Diacetyl monoxime thiosemicarbazide solution (DAM–TSC) solution (I) consists of 5 g diacetyl monoxime and 0.15 g thiosemicarbazide.

Random mutagenesis

Random mutations were introduced using error-prone PCR, which was carried out in 10 mM Tris–HCl (pH 8.3), 50 mM KCl, 0.01% (w/v) gelatin, 7 mM MgCl₂, 0.3 mM MnCl₂, 0.2 mM dATP, 0.2 mM dGTP, 1 mM dCTP, 1 mM dTTP, 10 pmol each primer (PpADI-fwd, 5'-AATTAATAC GACTCACTATAGGGGA-3', and PpADI-rev, 5'-GCTAGT TATTGCTCAGCGG-3'), 50 ng pET24a-ADI, and 2.5 U *Taq* DNA polymerase in a total volume of 50 μ l. The

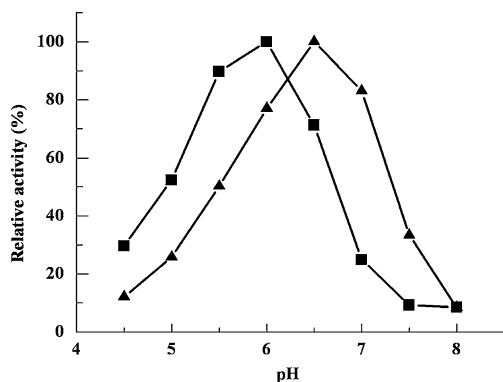


Fig. 3 Effect of pH on activity of the WT-ADI and M314. The activity is shown as percentages relative to that measured at optimum pH. Black square WT, black up-pointing triangle M314

plasmid pET24a-ADI (approximately 6.5 kb) carries PpADI encoding gene. The reaction mixture was heated at 94°C for 2 min, followed by 30 cycles of incubation at 94°C for 1 min, 52°C for 1 min, and 72°C for 2 min, and a final incubation at 72°C for 5 min. Amplification of the 1.5-kb product was checked by running a small aliquot of the reaction on an agarose gel.

Mutant library construction

Error-prone PCR reaction products were digested using *Nde*I and *Xho*I and purified by gel extraction. Expression vector pET 24a was also digested using *Nde*I and *Xho*I and purified by gel extraction. Digested ADI gene and pET 24a were ligated using T4 DNA ligase; the resulting plasmids were transformed into *E. coli* BL21 (DE3) for further expression and screening.

Colony activity assay by colorimetric 96-well microtiter plate screening

This method depicts a colorimetric 96-well microtiter plate activity assay for ADI by determining L-citrulline concentration. Single colonies were inoculated into the LB agar plate containing 30 μ g/ml kanamycin and 0.2 mM IPTG. The protein expression was performed by incubating at 30°C for 1 day, and colonies were picked into 96-well plates containing 50 μ l of sodium phosphate buffer (0.2 M, pH 7.4) with sterile toothpicks. A 50 μ l/well of 1 mM L-Arg phosphate buffer solution (same as above) was subsequently added and allowed to react at 37°C for 15 min, followed by addition of 90 μ l/well of acid-ferric reagent to terminate the reaction. After adding 30 μ l/well of DAM–TSC solution, the plate was incubated at 37°C for 2 h. Colonies with ADI activity result in formation of purple color with a λ_{\max} of 530 nm. The procedure for the screening of PpADI with improved activity is shown in Fig. 1.

Table 2 Activity and kinetic parameters of WT-ADI and M314

	pH 6.0		pH 7.4	
	<i>K_m</i> (mM)	Specific activity (U/mg)	<i>K_m</i> (mM)	Specific activity (U/mg)
WT	2.88	4.76	–	0.44
M314	0.43	16.7 (21.7 U/mg at pH 6.5)	0.65	9.02

Activity assay of ADI

The ADI activity was determined as previously described (Liu et al. 2008). Briefly, ADI was incubated with 20 mM arginine and 200 mM sodium phosphate buffer for 15 min at 37°C. Subsequently, acid-ferric solution was added to stop the enzyme reaction. After adding DAM–TSC solution, the mixture was boiled at 100°C for 10 min, and the optical density was measured at 530 nm. Protein concentration was determined using the Bradford reagent (Generay, CN) using bovine serum albumin as a standard. The expression and purification of rADI were confirmed by SDS-PAGE. One unit of rADI activity is defined as the amount of enzyme that required for converting 1 μmol of L-arginine into 1 μmol of L-citrulline per minute under the assay conditions.

Purification of recombinant ADI

The mutant was inoculated and cultured overnight at 37°C in 250-ml flasks containing 60 ml LB broth supplemented with 30 μg/ml kanamycin. The overnight culture was inoculated into fresh LB broth and was cultured at 37°C until the OD₆₀₀ was around 1.0. The recombinant ADI expression was induced by incubation with IPTG (0.2 mM) for 4 h at 30°C and then harvested by centrifugation (5,000×g, 6 min).

Cell pellets were resuspended in phosphate buffer (20 mM sodium phosphate, pH 7.4) and sonicated at 20 kHz for 5 min in an ice bath. The insoluble fraction was removed by centrifugation (4°C, 9,391×g, 20 min), and the supernatant was stored at 4°C as crude extracts for further purification. Crude extracts was subjected to anion ex-

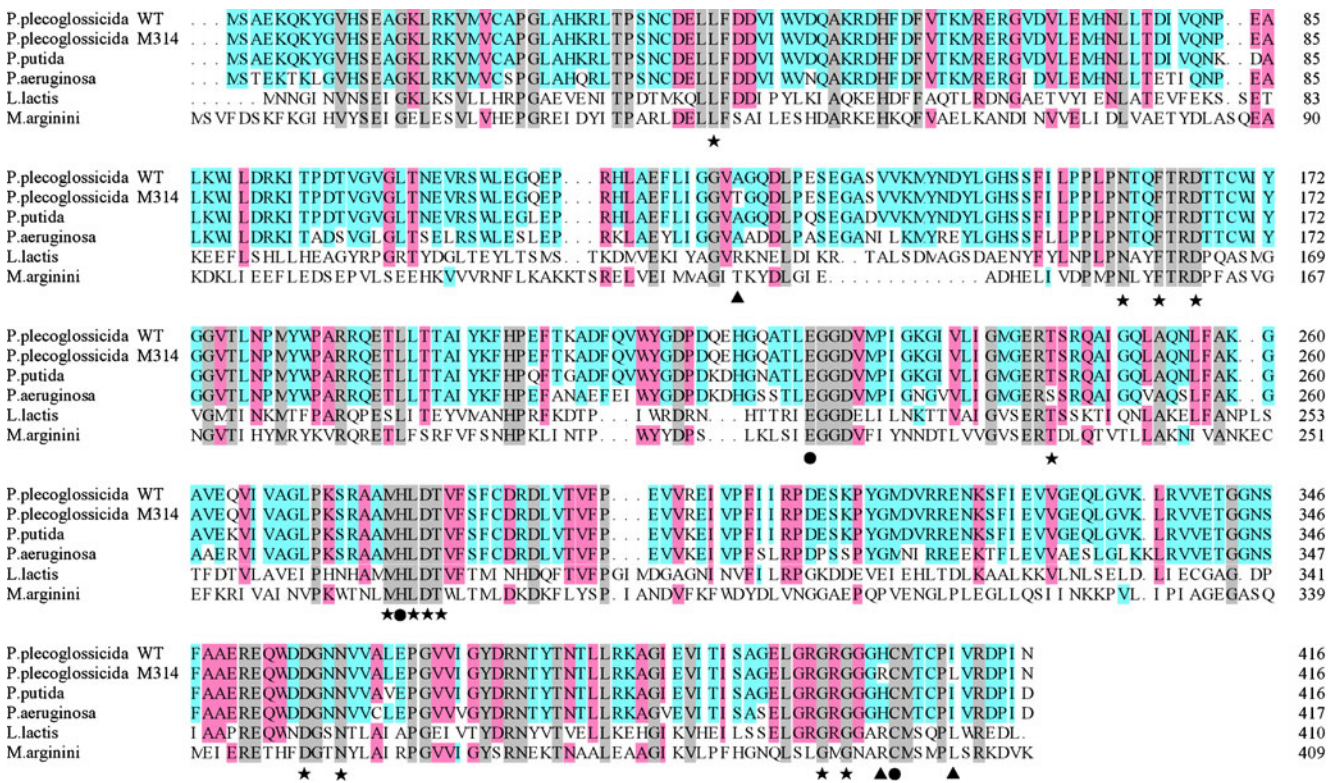


Fig. 4 Alignment of ADI protein sequences from *P. plecoglossicida* WT, *P. plecoglossicida* M314, *P. putida* (EAX15803), *P. aeruginosa* (X14694), *L. lactis* ssp. *lactis* (DQ364637), and *M. arginini* (X54141).

Mutation sites are marked with triangle. Key amino acids denoted with asterisks are involved in binding of the substrate, and amino acids marked with dots indicated the catalytic triad (Cys–His–Glu)

Table 3 Comparison of three amino acid substitutions and enzymatic properties of various ADIs

Source	Residues			Specific activity (U/mg)	Optimum pH	K_m (mM)	Identity (%)
	128	404	410				
<i>Pseudomonas plecoglossicida</i> (WT)	A	H	I	4.76	6.0	2.88	100
<i>Pseudomonas plecoglossicida</i> M314	T	R	L	21.7	6.5	0.43	99.3
<i>Pseudomonas putida</i>	A	H	I	58.8	6.0	0.2	96.4
<i>Pseudomonas aeruginosa</i>	A	H	I	NA	5.6	NA	84.7
<i>Lactococcus lactis</i>	R	R	L	143	7.2	8.7	31.6
<i>Mycoplasma arginini</i>	T	R	L	44.5	6.5	0.2	27.1

change chromatography on a HiPrep DEAE FF 16/10 column (GE Healthcare, Sweden), which had been pre-equilibrated with sodium phosphate buffer (20 mM, pH 7.4). Recombinant ADI was eluted by a NaCl gradient in same buffer at a rate of 2 ml/min. The obtained rADI protein was concentrated with Amicon Ultra-15 (10 kDa, Millipore, Bedford, MA, USA) and then subjected to Superdex 200 gel filtration column chromatography (GE Healthcare, Sweden). All the purifications were carried out using an ÄKTA explorer (Amersham).

Enzyme kinetics of recombinant ADI

K_m and V_{max} were determined using the above-described ADI activity assay method. Citrulline production was

quantified at various concentration of arginine (2, 4, 6, 8, and 10 mM). The pH dependence of enzyme activity was determined between pH 4.0 and 8.0 using 100 mM citric acid buffer (pH 4.0–5.0) and 200 mM sodium phosphate buffer (pH 5.5–8.0). The activity was then measured using the method described above.

Molecular modeling

In order to better understand the relationship between enzymatic properties and amino acid sequence, a homology model of M314 based on crystal structures of PaADI (PDB codes: 1RXX) was constructed by SWISS-MODEL homology-modeling web server (www.expasy.ch/tools) (Schwede et al. 2003). One monomeric unit of the tetrameric PaADI was used for the modeling study.

Results

Directed evolution of PpADI

The WT-ADI exists as a homodimer in the native condition and catalyzes the irreversible hydrolysis of arginine to citrulline and ammonia. The specific activity of WT-ADI was determined to be 4.76 U/mg at pH 6.0 and 37°C. An acidic pH optimum of 6.0 was observed, a pH shift from 6.0 to 7.4 results in over 90% activity drop (Ni et al. 2009). Typical directed evolution strategy ep-PCR combined with high-throughput screening was applied to obtain PpADI variants with increased specific activity and decreased K_m at physiological pH (Fig. 1). Transformants of mutant library was induced on IPTG-agar plates and directly subjected to the activity assay by picking colonies into 96-well plate (Fig. 1). After screening 650 clones by colorimetric 96-well microtiter plate method, eight variants exhibiting increased ADI activity at pH 7.4 were identified. The activities of improved mutants were further confirmed by liquid cultivation in shake flasks. Crude extracts of these mutants were prepared by sonication and centrifugation,

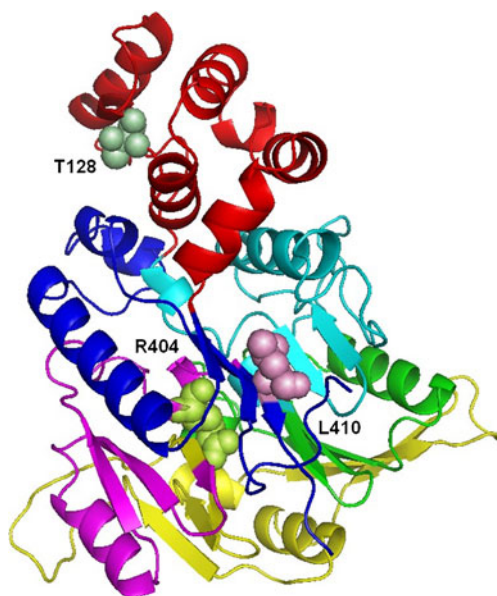


Fig. 5 Overall fold of PpADI M314. Three residues mutated are colored pale cyan (T128), lime green (R404), and pink (L410L), and displayed as spheres. Stereoscopic view of the fold and highlights the fivefold pseudosymmetry with five modules depicted in different colors: blue I (residues 7–72, 408–417); red α -helical domain (residues 73–157); cyan II (residues 158–227); green III (residues 228–282); yellow IV (residues 283–361); magenta V (residues 362–407)

and the ADI activity was measured at both pH 7.4 and 6.0. Three mutants (M177, M314, and M558) with 4.77-, 8.64-, and 20.5-folds increased activity at pH 7.4 were selected for sequence analysis to determine the mutations conferring the desired features. The results show that both M177 (V107) and M558 (R18L) harbor one amino acid mutation, while three substitutes were identified in M314 (A128T, H404R, I410L) (Table 1). M314 exhibiting the highest activity at pH 7.4 was selected for subsequent purification and characterization.

Purification and enzymatic properties of mutant 314

The PpADI M314 was expressed and purified to homogeneity using DEAE FF anion exchange and Superdex 200 gel filtration column chromatography. As expected, the molecular weight of rADI was calculated to be 92.6 kDa by gel filtration (Fig. 2b) and approximately 46 kDa using SDS-PAGE (Fig. 2a, lane 3). It was assumed that M314 consists of two apparently identical subunits (46.3 kDa).

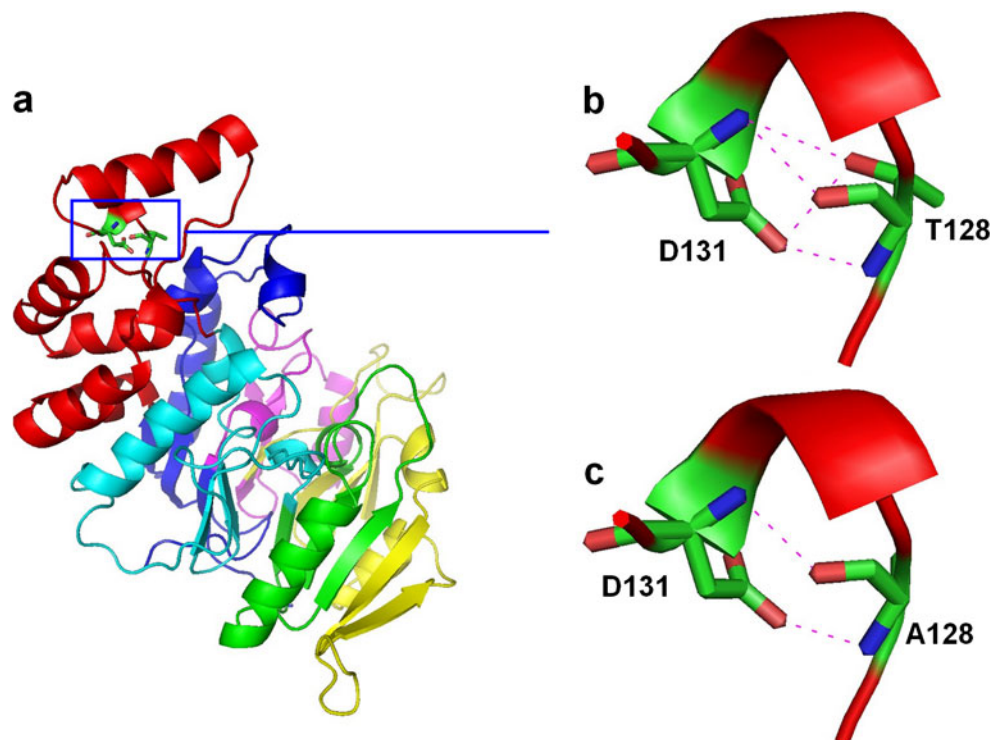
As shown in Fig. 3, the pH optimum shifts from 6.0 to 6.5 in M314. The K_m value estimated from the Lineweaver–Burk plots was 2.88 mM for WT-ADI and 0.65 for M314 (pH 7.4). The specific activity of ADI from M314 is 9.02 U/mg, representing over 20-fold increase compared with WT-ADI (0.44 U/mg) at pH 7.4 (Table 2).

Homology modeling of mutant 314

Amino acid sequence of PpADI M314, WT-ADI (EU030267), and ADIs from *Pseudomonas putida* (EAX15803), *Pseudomonas aeruginosa* (X14694), *Lactococcus lactis* ssp. *lactis* (DQ364637), and *Mycoplasma arginini* (X54141) were aligned using DNAMAN software packages (version 5.2.9; Lynnon Biosoft, Quebec, Canada) to compare three substitutions in M314 (A128T, H404R, I410L) (Fig. 4). Three amino acid residues of above ADIs and their enzymatic properties including specific activity, pH optimum, and K_m were summarized in Table 3. M314 has improved pH optimum (6.0–6.5), lower K_m (2.88 to 0.43 and 0.65 mM), and 4.6-fold increase in specific activity at its optimal pH. It is noticed that 128A, 404H, and 410I are conserved in *Pseudomonas* ADIs (Shibatani et al. 1975; Galkin et al. 2004) with acidic pH optimum (5.6–6.0). Interestingly, despite their low sequence identity (27.1%), three amino acid substitutes in M314 are coincident with corresponding residues in *M. arginini* ADI, which is prominent for its low K_m (0.2 mM) and high specific activity (44.5 U/mg) at pH 6.5 (Takaku et al. 1992). In addition, residues 404R and 410L were found to be identical with those in *L. lactis* ADI (Kim et al. 2007), which has a strikingly high activity of 143 U/mg at pH 7.2 and also a low homology (31.6%) to M314.

A BLAST search of the NCBI database with M314 revealed that best match is arginine deiminase from *P. aeruginosa* (PaADI). The highest similarity (84.2%) was

Fig. 6 Stereoscopic view of mutation A128T in PpADI. **a** Overall fold of PpADI M314. **b** Hydrogen bonds between T128 and D131. **c** Hydrogen bonds between A128 and D131



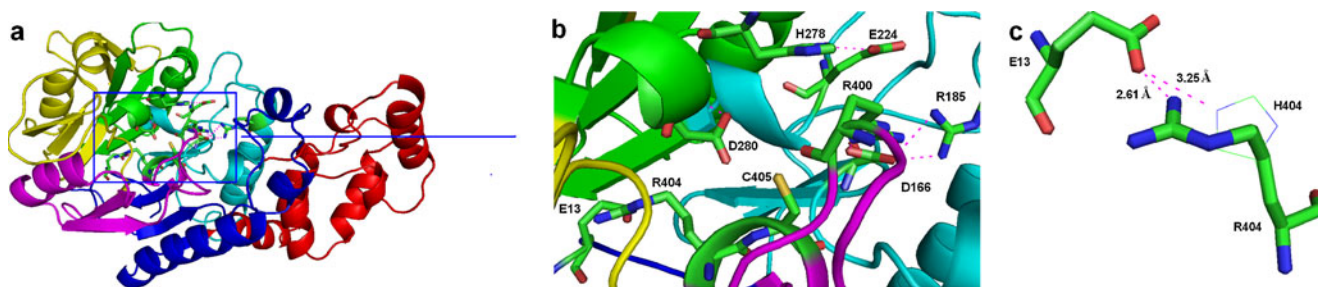


Fig. 7 Stereoscopic view of mutation H404R in PpADI. **a** Overall fold of PpADI M314. **b** Stereoscopic view of key residues around H404R substitution. **c** Distance of hydrogen bond between H404R and E13

found with *P. aeruginosa* ADI whose X-ray structure has been solved at 2.45 Å (Galkin et al. 2004). In order to better understand the molecular mechanism of M314, a homology model of M314 based on *P. aeruginosa* ADI structure (PDB No. 1RXX) was constructed by SWISS-MODEL (Schwede et al. 2003). The predicted structure of M314 is similar to PaADI, in a fivefold $\beta\beta\alpha\beta$ pseudosymmetrical barrel arrangement, as well as an additional α -helical domain comprising five α -helices at the same position (Fig. 5). The molecular role of the amino acid substitutes in M314 was analyzed based on their effects on the protein structure and properties in the homology model.

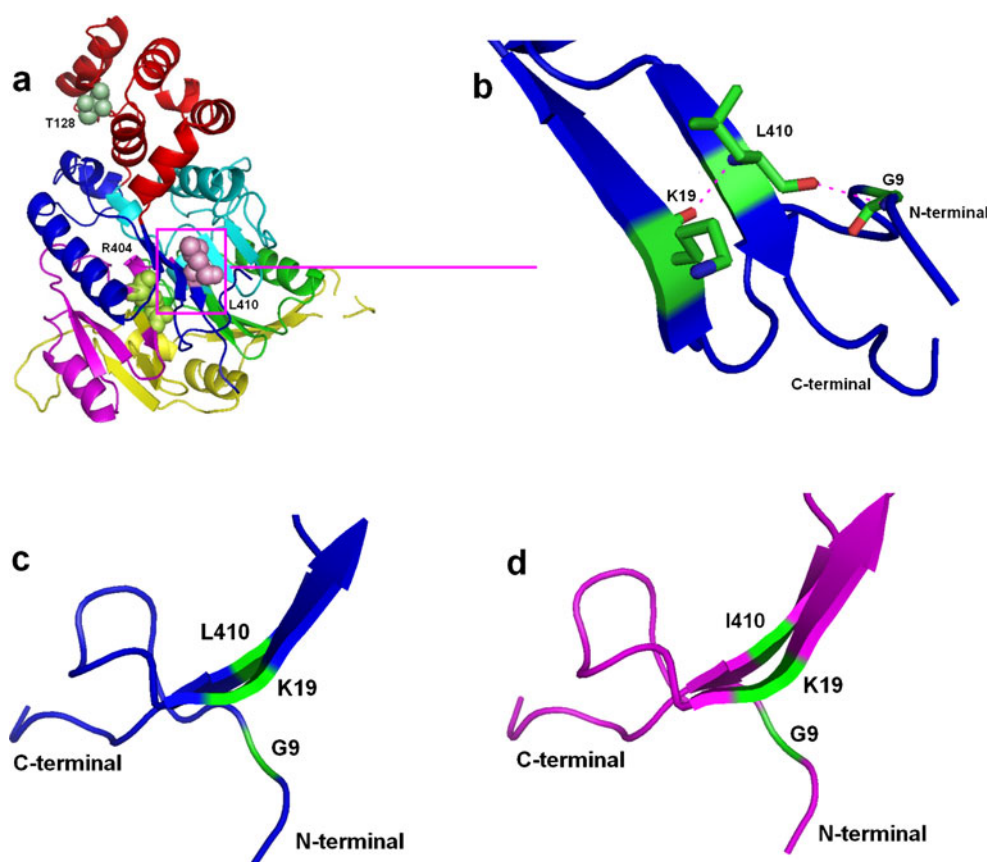
Mutation A128T locates in the loop between the fourth and fifth α -helices in α -helical domain, followed by a small

α -helix formed by 129G, 130Q, and 131D (Fig. 6a). In M314, the hydroxyl group of Thr128 engages in hydrogen bond interaction with both amino and carboxyl group of Asp131, resulting four hydrogen bonds in total (Fig. 6b), while two hydrogen bonds are formed between Ala128 and Asp131 in WT-ADI (Fig. 6c).

It is observed that the imidazole group of H404 is engaged in the hydrogen bond interaction with the carboxyl group of E13, and distance of H bond is estimated to be 3.25 Å. In H404R mutant, a shorter hydrogen bond between guanidino group of Arg404 and Glu13 (2.61 Å) is observed, favoring a more stable interaction between them (Fig. 7c).

In the characteristic fivefold pseudosymmetric structure of PpADI, the first module is extended to topology $\beta\beta\beta\alpha\beta$ and

Fig. 8 Stereoscopic view of mutation I410L in PpADI. **a** Overall fold of PpADI M314. **b** Hydrogen bonds between L410 and K19, G9. **c** β -sheets in C- and N-terminal after I410L mutation. **d** β -sheets in C- and N-terminal before I410L mutation



composed by the last β sheet in C-terminal (residues 408–417) and the first $\beta\beta\alpha\beta$ unit in N-terminal (residues 6–71) (Fig. 8a). Leu410, a C-terminal residue inside the protein, forms hydrogen bonds with amino group of Gly9 and carboxyl group of Lys19 (Fig. 8b), leading a close connected C-terminal β -sheet and the first β -sheet in N-terminal. It is observed that I410L substitution causes a twisted β -sheet towards N-terminal (Fig. 8c, d), which might due to the electron cloud difference between Ile and Leu.

Discussion

In this study, directed evolution was demonstrated to be effective in improving the activity and K_m of PpADI under physiological pH. Using lower substrate concentration and appropriate reaction system, a sensitive and precise 96-well plate screening strategy based on a modified DAM–TSC method was developed for isolating ADI variants with higher specific activity and lower K_m . Additionally, the tedious liquid cultivation was replaced by IPTG-agar plate, which was conveniently combined with 96-well plate activity assay. Employing this two-step screening procedure, M314 was selected from 650 variants after one round of ep-PCR, exhibiting over 20-fold increased activity and lower K_m . A $MnCl_2$ concentration of 0.3 mM was used in ep-PCR, generating average 1–3 amino acid substitutions per gene and 55.2% inactive clones. Arnold's group shows that an optimum mutation rate could balance the relationship between production of unique sequences and retention of enzyme functionality (Drummond et al. 2005).

In the homology model of M314 constructed based on PaADI, it is also noticed that the amino acid sequence of α -helical domain in M314 shares 74.4% identity with that of PaADI. Differing from PaADI tetramer, SDS-PAGE and gel filtration analysis indicated that M314 has a homodimer structure (Fig. 2), same as its parent (Ni et al. 2009). It is therefore speculated that some critical residues in α -helical domain might be responsible for the formation of either tetramer or dimer, which awaits further study.

The molecular mechanism of three substitutes in M314 was analyzed in the stereoscopic structure of PpADI. In A128T, the stronger hydrogen bond renders higher stability in the small α -helix (129–131). Additionally, as a residue on the exterior surface of PpADI, the replacement of hydrophobic Ala with hydrophilic Thr could possibly improve its interaction with the aqueous environment. The I410L substitute confers a closer linkage between β -sheets of C- and N-terminal in M314, and presumably a more stable N-terminal of the protein.

It was reported that in PaADI, the Asp280 carboxylate group interacts with the imidazole group of His405, which in turn interacts with Glu13. Asp280 was proposed to be a

general base in the reaction mechanism of PaADI; it interacts with substrate (arginine) guanidinium group and is important for substrate binding (Galkin et al. 2005). His404 (imidazole group pKa 6.0) is protonated in acidic pH and become deprotonated in physiological pH, whereas Arg404 (guanidine group pKa 12.48) remains protonated. A protonated Arg404 can form a hydrogen bonding with Asp280 and favor substrate interactions at physiological pH, when His404 becomes deprotonated. The H404R substitute may therefore explain the higher pH optimum of M314, and the H404R mutant was used as starting variant in the directed evolution of PpADI previously (Zhu et al. 2010). On the other hand, position 404 locates right next to one of the catalytic center residues Cys405 (Fig. 7b); the extension of Arg404 towards Glu13 (Fig. 7c) could help reduce the space hindrance effect in the substrate binding and catalytic center, thereby enhance the substrate affinity of PpADI.

In this study, the specific activity of M314 is improved for over 20 times at pH 7.4 compared with WT-ADI, and its pH optimum is shifted from 6.0 to 6.5. The pH profile of M314 is however far from satisfactory, since merely 41% of the activity at pH 6.5 is retained at physiological pH 7.4 (Table 2). To further improve the enzymatic properties of ADI as an anti-tumor drug, the second round of directed evolution is currently undergoing. Also, site-directed mutagenesis is being carried out to understand the effects of single amino acid substitution and its molecular mechanism in the enzymatic activity.

Taken together, an efficient directed evolution procedure has been established to improve the activity of ADI under physiological pH. After one round of ep-PCR, an excellent mutant 314 was selected, which shows over 20-fold increased specific activity, significantly reduced K_m (2.88 to 0.43 and 0.65 mM), and a shifted pH optimum towards physiological condition (from pH 6.0 to 6.5). This work could provide potent candidates for developing an anti-tumor drug for arginine-auxotrophic cancers including melanomas and HCCs.

Acknowledgements This research was supported by Natural Science Foundation of China (30900030), Research Fund for the Doctoral Youth Scholars Program of Higher Education of China (20090093120008), and the Program of Introducing Talents of Discipline to Universities, No. 111-2-06.

References

- Archibald RM (1944) Determination of citrulline and allantoin and demonstration of citrulline in blood plasma. *J Biol Chem* 156:121–142
- Curley SA, Cusack JC, Tanabe KK, Elis LM (2002) Advances in the treatment of liver tumors. *Curr Probl Surg* 39:449–572

- Drummond DA, Iverson BL, Georgiou G, Arnold FH (2005) Why high-error-rate random mutagenesis libraries are enriched in functional and improved proteins. *J Mol Biol* 350:806–816
- Galkin A, Kulakova L, Sarikaya E, Lim K, Howard A, Herzberg O (2004) Structural insight into arginine degradation by arginine deiminase, an antibacterial and parasite drug target. *J Biol Chem* 279:14001–14008
- Galkin A, Lu X, Dunaway-Mariano D, Herzberg O (2005) Crystal structures representing the Michaelis complex and the thiouronium reaction intermediate of *Pseudomonas aeruginosa* arginine deiminase. *J Biol Chem* 280:34080–34087
- Gong H, Zölzer F, von Recklinghausen G, Rössler J, Breit J, Havers W, Fotsis T, Schweigerer L (1999) Arginine deiminase inhibits cell proliferation by arresting cell cycle and inducing apoptosis. *Biochem Biophys Res Commun* 261:10–14
- Gong H, Zölzer F, von Recklinghausen G, Havers W, Schweigerer L (2000) Arginine deiminase inhibits proliferation of human leukemia cells more potently than asparaginase by inducing cell cycle arrest and apoptosis. *Leukemia* 14:826–829
- Izzo F, Marra P, Beneduce G, Castello G, Vallone P, Rosa VD, Cremona F, Ensor CM, Holtsberg FW, Bomalaski JS, Clark MA, Ng C, Curley SA (2004) Pegylated arginine deiminase treatment of patients with unresectable hepatocellular carcinoma: results from phase I/II studies. *J Clin Oncol* 22:1815–1822
- Kim JE, Jeong DW, Lee HJ (2007) Expression, purification, and characterization of arginine deiminase from *Lactococcus lactis* ssp. *lactis* ATCC 7962 in *Escherichia coli* BL21. *Protein Expr Purif* 53:9–15
- Kim RH, Coates JM, Bowles TL, McNerney GP, Sutcliffe J, Jung JU, Edwards RG, Chuang FYS, Bold RJ, Kung HJ (2009) Arginine deiminase as a novel therapy for prostate cancer induces autophagy and caspase-independent apoptosis. *Cancer Res* 69:700–709
- Kuo MT, Niramol S, Feun LG (2010) Targeted cellular metabolism for cancer chemotherapy with recombinant arginine-degrading enzymes. *Oncotarget* 1:246–251
- Lin L, Meng X, Liu PF, Hong YZ, Wu GB, Huang XL, Li CC, Dong JL, Xiao L, Liu ZD (2009) Improved catalytic efficiency of endo- β -1,4-glucanase from *Bacillus subtilis* BME-15 by directed evolution. *Appl Microbiol Biotechnol* 82:671–679
- Liu YM, Sun ZH, Ni Y, Zheng P, Liu YP, Meng FJ (2008) Isolation and identification of an arginine deiminase producing strain *Pseudomonas plecoglossicida* CGMCC2039. *World J Microbiol Biotechnol* 24:2213–2219
- Miyazaki K, Takaku H, Umeda M, Fujita T, Huang WD, Kimura T, Yamashita J, Horio T (1990) Potent growth inhibition of human tumor cells in culture by arginine deiminase purified from a culture medium of a *Mycoplasma*-infected cell line. *Cancer Res* 50:4522–4527
- Ni Y, Li ZW, Sun ZH, Zheng P, Liu YM, Zhu LL, Schwaneberg U (2009) Expression of arginine deiminase from *Pseudomonas plecoglossicida* CGMCC2039 in *Escherichia coli* and its anti-tumor activity. *Curr Microbiol* 58:593–598
- Qian JN, Sun ZH, Liu YP, Meng FJ, Liu YM (2007) Determination of L-citrulline in enzymatic conversion solution by diacetylmonoxime–thiosemicarbazide colorimetry. *Chin J Pharm* 38:519–521 (in Chinese)
- Ryder SD (2003) Guidelines for the diagnosis and treatment of hepatocellular carcinoma (HCC) in adults. *Gut* 52:iii1–iii8
- Schwede T, Kopp J, Guex N, Peitsch MC (2003) SWISS-MODEL: an automated protein homology-modeling server. *Nucleic Acids Res* 31:3381–3385
- Shen LJ, Shen WC (2006) Drug evaluation: ADI-PEG-20-a PEGylated arginine deiminase for arginine-auxotrophic cancers. *Curr Opin Mol Ther* 8:240–248
- Shibatani T, Kakimoto T, Chibata I (1975) Crystallization and properties of L-arginine deiminase of *Pseudomonas putida*. *J Biol Chem* 250:4580–4583
- Shirai H, Blundell TL, Mizuguchi K (2001) A novel superfamily of enzymes that catalyze the modification of guanidino groups. *Trends Biochem Sci* 26:465–468
- Sugimura K, Ohno T, Fukuda S, Wada Y, Kimura T, Azuma I (1990) Tumor growth inhibitory activity of a lymphocyte blastogenesis inhibitory factor. *Cancer Res* 50:345–349
- Sugimura K, Ohno T, Kusuyama T, Azuma I (1992) High sensitivity of human melanoma cell lines to the growth inhibitory activity of mycoplasmal arginine deiminase in vitro. *Melanoma Res* 2:191–196
- Takaku H, Takase M, Abe SI, Hayashi H, Miyazaki K (1992) In vivo anti-tumor activity of arginine deiminase purified from *Mycoplasma arginini*. *Int J Cancer* 51:244–249
- Takaku H, Misawa S, Hayashi H, Miyazaki K (1993) Chemical modification by polyethylene glycol of the anti-tumor enzyme arginine deiminase from *Mycoplasma arginini*. *Jpn J Cancer Res* 84:1195–1200
- Takaku H, Matsumoto M, Misawa S, Miyazaki K (1995) Anti-tumor activity of arginine deiminase from *Mycoplasma arginini* and its growth-inhibitory mechanism. *Jpn J Cancer Res* 86:840–846
- Watkins KY, Curley SA (2000) Liver and bile ducts. In: Abeloff MD, Armitage JO, Lichter AS, Neiderhuber JE (eds) *In clinical oncology*, 2nd edn. Churchill Livingstone, New York, pp 1681–1748
- Zhu L, Tee KL, Roccatano D, Sonmez B, Ni Y, Sun ZH, Schwaneberg U (2010) Directed evolution of an antitumor drug (arginine deiminase PpADI) for increased activity at physiological pH. *Chembiochem* 11:691–697